Photoelectrocatalytic degradation of chlortetracycline using Ti/TiO$_2$ nanostructured electrodes deposited by means of a Pulsed Laser Deposition process

Rimeh Daghrir [a,1], Patrick Drogui [a,*], Ibrahima Ka [b,2], My Ali El Khakani [b,3]

[a] Institut national de la recherche scientifique, Centre Eau, Terre et Environnement, 490 rue de la Couronne, Québec, Qc, Canada, G1K 9A9
[b] Institut national de la recherche scientifique, INRS-Énergie, Matériaux et Télécommunications, 1650 Blvd. Lionel-Boulet, Varennes, Qc, Canada, J3X 1S2

ARTICLE INFO

ABSTRACT

Ti/TiO$_2$ electrode was prepared by means of the Pulsed Laser Deposition method and used in a photo-electrocatalytic oxidation (PECO) process in order to degrade chlortetracycline (CTC). The deposited TiO$_2$ coatings were found to be of rutile structure. High treatment efficiency of CTC was achieved by the PECO process compared to the conventional electrochemical oxidation, direct photolysis and photocatalysis processes. Several factors such as current intensity, treatment time, UV lamp position and initial concentration of CTC were investigated. Using a 2^4 factorial matrix, the best performance for CTC degradation (74.3% of removal) was obtained at a current intensity of 0.5 A during 120 min of treatment time and when the UV lamp was immersed in the solution in the presence of 25 mg L^{-1} of CTC. The current intensity and treatment time were the main parameters influencing the degradation rate of CTC. Subsequently, a central composite design methodology has been investigated to determine the optimal experimental parameters for CTC degradation. The PECO process applied under optimal conditions (at current intensity of 0.39 A during 120 min with internal position of the UV lamp) is able to oxidize around 74.2 ± 0.57%, of CTC.

© 2011 Elsevier B.V. All rights reserved.

1. Introduction

In the past few years, there has been considerable interest to pharmaceuticals and personal care products (PPCPs) including antibiotics, hormones, anesthetics, etc. due to their discharges into the environment. These contaminants are soluble in surface water, groundwater, and even drinking water [1–4]. Antibiotics belong to pharmaceutical compounds most often used as growth promoters of animals. The discharge of antibiotics into the environment is one of the major and global public health issues that need urgent action. Its annual usage has been globally estimated between 100,000 and 200,000 tones [5]. Chlortetracycline (CTC); oxytetracycline (OTC); and tetracycline (TC) are the most often used throughout the world [1,6–8]. Antibiotics or their metabolites have been detected in surface water, ground water, sewage water, and drinking water at concentrations ranging from ng L^{-1} to μg L^{-1} [1,9,10]. These findings have raised concern regarding potential human health effects caused by low levels of antibiotics in drinking water, as well as the transfer and spread of antibiotic resistant genes among microorganisms [11]. Globally, a very low proportion (<1%) of these antibiotic compounds participates to the total DOC from pollutants in contaminated water, but their presence in water has to be taken into account owing to their potential toxicity for human. Thus, it is of great importance to develop efficient and cost-effective treatment technologies for removal of such compounds.

Conventional wastewater treatments such as traditional biological treatment methods are not always able to remove completely antibiotic compounds [1,12]. It has been found by Ingerslev and Halling-Sorensen [13] that twelve sulfonamide antibiotics were not readily biodegradable in activated sludge. Likewise, Kummerer and Hartmann [14] investigated the effectiveness of the treatment of hospital and pharmaceutical wastewaters in several wastewater treatment plants in Germany. These works showed that many pharmaceutical products could not be oxidized during conventional biological treatments. However, other methods can be used to remove antibiotics such as adsorption, biosorption, ozonation, membrane techniques (reverse osmosis), advanced oxidation processes (AOPs), including O$_3$/H$_2$O$_2$, UV/O$_3$, UV/H$_2$O$_2$, H$_2$O$_2$/Fe^{2+},

Nomenclature

ANOVA	analysis of variance
AOPs	advanced oxidation processes
CB	conduction band
CCD	central composite design
CTC	chlortetracycline
DP	direct photolysis
EO	electro-oxidation
FD	factorial design
LC/MS/MS	liquid chromatograph/mass spectrophotometer/mass spectrophotometer
PC	photocatalysis
PECO	photoelectrocatalytic oxidation
PLD	Pulsed Laser Deposition
PPCPs	pharmaceuticals and personal care products
R^2	regression coefficient
RSM	response surface methodology
SEM	scanning electron microscopy
VB	valance band
XRD	X-ray diffraction
XPS	X-ray photoelectron spectroscopy

Fig. 1. Schematic diagram of the photoelectrocatalytic reactor: (1) DC power supply, (2) quartz window, (3) UV lamp, (4) photometer, (5) photoanode, (6) cathode, (7) stirring bar, and (8) magnetic stirrer.

etc. [1,15–17]. Among them, chemical oxidation processes have been successfully applied to degrade various pharmaceutical compounds present in contaminated water. UV and UV/H_2O_2 oxidation processes are used to degrade three antibiotics from tetracycline group (tetracycline; chlortetracycline; and oxytetracycline) [1]. In spite of the good oxidation of refractory organic pollutants, the complexity of these methods (advanced oxidation processes), high chemical consumption, and relatively high treatment costs constitute major barriers for large-scale applications [18].

In the same context, photocatalysis process combining UV and TiO_2 suspensions as catalyst was used by Reyes et al. [12] to degrade tetracycline as a model of antibiotic compounds. Degradation around 50% was recorded after 10 min of treatment using $0.5 \, g \, L^{-1}$ of TiO_2 exposed to UV light. A renewed interest in photocatalysis has been spurred by the search for reliable, cost-effective water treatment processes. From this point of view, it can be interesting to develop photoelectrocatalytic oxidation (PECO) technique combining electrolytic and photocatalytic processes. This approach offers the possibility to delay the recombination of the electron–hole pairs (e^-_{CB}/h^+_{VB}) and the possibility to increase the lifetime of the latter. The applied external potential in PECO technique is the key factor because it accelerates the photocatalytic reaction.

The aim of the present study is to evaluate the efficiency of a PECO process using UV light and nanocrystalline TiO_2 photo-anodes for the efficient treatment of waters contaminated by CTC. To this end, an experimental design methodology [19] was put in place to investigate the influence of the principal experimental parameters (current intensity, treatment time, pollutant concentration, and UV lamp position) on the efficiency of the PECO process for CTC degradation. A second objective of this study was to use a statistical methodology for a rational analysis of the combination of operational factors that led to the best treatment process. Factorial design (FD) and central composite design (CCD) methodologies have been successively applied in order to point out the main and interaction effects of the factors and to optimize CTC degradation by the PECO process.
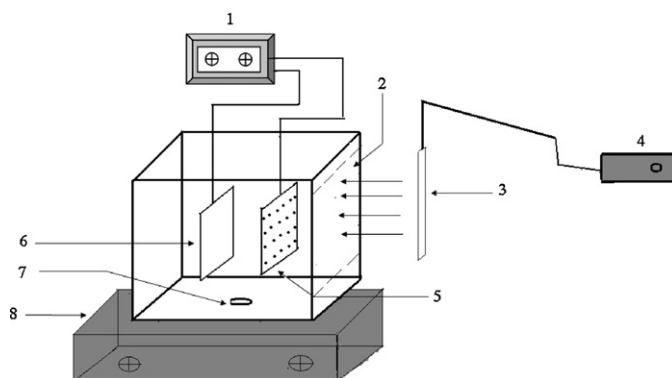
2. Materials and methods

2.1. Ti/TiO$_2$ electrode preparation

The titanium dioxide (TiO_2) coatings have been performed by means of a Pulsed Laser Deposition (PLD) method. A KrF excimer laser (wavelength = 248 nm, pulse duration = 15 ns) operating at a repetition rate of 30 Hz was focused, at an incidence angle of 45°, onto the TiO_2 rotating target (99.95% purity). The on-target laser energy density was set to $4.5 \, J/cm^2$. The TiO_2 films were deposited on both titanium grids (for photoelectrochemical studies) and on silicon substrates (for material characterizations purposes). The TiO_2 deposits were performed at a deposition temperature 600 °C under an oxygen background pressure of 1 mTorr. The PLD deposition chamber was first turbo-pumped to about 10^{-6} Torr before filling it with oxygen. More details on the Pulsed Laser Deposition system and it schematics can be found elsewhere [20].
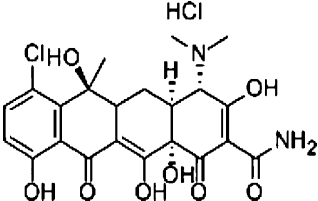
2.2. Preparation of the synthetic solution

Chlortetracycline hydrochloride ($C_{22}H_{24}Cl_2N_2O_8$) was an analytical grade reagent supplied by Sigma Aldrich (purity 78%). Its water solubility was $0.008 \, mol \, L^{-1}$ [1]. Table 1 presents some chemicals properties of CTC [21]. CTC stock solution was prepared in a glass-tank containing 2 L of distilled water in which 100 mg of CTC was added. Solubilization of CTC was carried out at a high speed of 750 rpm for a 30 min. Mixing was achieved by a Teflon-covered stirring bar installed at the bottom of the beaker. Final concentration of CTC was $50 \, mg \, L^{-1}$. In order to increase electrical conductivity in the solution, $0.05 \, mol \, L^{-1}$ of sodium sulfate was added.

2.3. Experimental devices

The reactor unit was made of acrylic material with a dimension of 12.7 cm (width), 16.51 cm (length), and 11.43 cm (depth). A quartz window (8.89 cm × 8.89 cm) was disposed on one face of the reactor for the photoelectrocatalysis experiments (Fig. 1). All the assays were conducted in batch mode. The photoelectrocatalytic cell was comprised of one anode (Ti/TiO$_2$) and one cathode (inox), each one having a surface area of $110 \, cm^2$ (10 cm width × 11 cm high), placed in parallel and were submerged in the solution. The electrodes were vertically installed on a perforated Plexiglas plate placed at 2 cm from the bottom of the cell. The inter-electrode gap was 1.0 cm. Both anode and cathode were connected respectively to the positive and negative outlets of a DC power supply Xantrex XFR 40-70 (Aca Tmetrix, Mississauga, ON, Canada) with a maximum current rating of 70 A at an open circuit potential of 40 V. The photoelectrocatalytic cell was operated with current intensities (from

Table 1
Chemical properties of chlortetracycline hydrochloride.

Molecule	Molecular formula	Chemical structure	Molecular weight ($g\,mol^{-1}$)	Solubility ($mol\,L^{-1}$)	pK_{a1}[a]	pK_{a2}[a]	pK_{a3}[a]
CTC	$C_{22}H_{24}Cl_2N_2O_8$		515.3	0.008	3.3 ± 0.3	7.55 ± 0.02	9.3 ± 0.3

[a] pK_a was determined by Qiang and Adams (2004).

0.16 A to 0.59 A) imposed during treatment period ranging from 40 to 120 min. The photo-anode was illuminated by a mercury lamp (light intensity = 6.9 mW cm^{-2}; λ_{max} = 254 nm) through the quartz window. The lamp was installed vertically outside or inside the reactor. The light intensity was measured with a photometer (Model PS-3, 99-0057-01, UVp Company; USA). The photoelectrocatalytic reactor was placed in a dark chamber in order to avoid interferences from the daylight. Mixing in the cell was achieved by a Teflon-covered stirring bar installed between the perforated plate and the bottom of the cell. All experiments were carried out at room temperature (25 °C). For all tests a total volume of 1.0 L was used. An electrolyte concentration of 0.05 mol $Na_2SO_4\,L^{-1}$ was added in the synthetic solution. Sodium sulfate was analytical grade reagent and supplied by Mat Laboratory (Quebec, Qc, Canada).

2.4. Experimental design

Response surface methodology (RSM) was applied to evaluate and determine the optimum operating conditions. RSM is a collection of mathematical and statistical methods for modeling, optimizing, and analyses a treatment process in which the response can be influenced by several variables [22]. Both factorial design (FD) and central composite design (CCD) methodologies are widely used in RSM. FD was used in order to investigate the main and interaction effects of the factors on the degradation of CTC. Subsequently, CCD was employed to optimize PECO process in CTC degradation. A four-factorial and a two-level central composite design, with six replicate at the center point for each categorical factor, led to a total number of forty experiments employed for response surface modeling. The variables investigated in our study were: the applied current intensity ($X1$), treatment time ($X2$), pollutant concentration ($X3$), and UV lamp position ($X4$). CTC degradation efficiency was considered as response (Y). The values of different variables were selected based on the preliminary assays.

2.5. Analytical details

The pH was determined using a pH-meter (Fisher Acumet model 915) equipped with a double-junction Cole-Palmer electrode with Ag/AgCl reference cell. The progress of photoelectrocatalysis degradation of CTC in the solution was firstly monitored by absorbance measurements using UV–vis absorption spectrophotometer (UV 0811 M136, Varian, Australia). The maximum absorption of the solution samples has been made at the wavelength of 368 nm in an optical quartz cell (1 cm). This absorption peak was chosen to evaluate the residual CTC concentration. A calibration curve of known CTC concentration versus absorbance (368 nm) was used to calculate the residual CTC concentrations.

Likewise, the progress of photoelectrocatalytic degradation of CTC was monitored and quantified by LC/MS/MS (Thermo TSQ Quantum Access). The chromatographic column used was Hypersil Gold C18, particle size 3 μm and 2.1 × 100 mm inner diameter. The isocratic mobile phase was A: 50% H_2O + 0.1% formic acid and B: 50% CH_3CN + 0.1% formic acid at a flow rate of 200 μL min^{-1}. Mass spectral data shown in this study were acquired on a LCQ Duo ion trap tandem mass spectrometry equipped with an electrospray ionization (ESI) source operated in positive ion mode. Qualitative analysis of CTC was determined using standard addition method (SAM). SAM is based on the addition of small known quantities of analyte to the sample [23]. The calibration curve of five points (from 0.1 mg L^{-1} to 20 mg L^{-1}) was prepared from a stock solution 20 mg L^{-1}. A certified control was prepared at concentration of 5 mg L^{-1} in the center of the curve. The percentage of recovery of the analyte at the end of the analysis was 83%.

2.6. Economic aspect

The economic study included chemical and energy consumption. The electric cost was estimated about of US$0.06 kW h^{-1}. A unit cost of US$0.30 kg^{-1} was used of electrolyte (Na_2SO_4 industrial grade). The total cost was evaluated in terms of U.S. dollars spent per cubic meter of treated solution (US$ m^{-3}).

3. Results and discussion

3.1. Characterization of the Ti/TiO$_2$ electrode

The surface morphology of the TiO$_2$ photocatalytic coating was examined by SEM observations. Fig. 2a shows the top-view of the TiO$_2$ film deposited at 600 °C onto silicon substrate. The coating is seen to be highly dense with fine-grained surface with more or less spherical features of few tens of nm of diameter (as shown in the higher magnification SEM image of Fig. 2b). The cross-sectional SEM views reveal the columnar growth of the TiO$_2$ coating where The TiO$_2$ columns are seen to be densely packed (Fig. 2d). Fig. 2c also shows that the TiO$_2$ coating is very uniform in thickness and forms a very smooth and continuous interface with the underlying substrate. The XRD analysis (Fig. 3) indicates that our TiO$_2$ coatings deposited at 600 °C are polycrystalline and crystallize in the TiO$_2$ rutile phase, in accordance with literature data where the TiO$_2$ rutile phase is generally obtained for deposition temperatures above 550 °C [24–26]. The XRD spectrum of the TiO$_2$ coating onto the Ti-grid confirms the presence of the same TiO$_2$ rutile phase obtained on Si. The average size of the TiO$_2$ crystallites was estimated to about 29 nm on silicon while it is of ~10 nm on the Ti-grid substrates. Such a nanometric grain size is expected to have an important effect on the photocatalytic activity of the TiO$_2$ coating [27,28]. Indeed, with the decrease in particle size, the catalytic activity is enhanced due to the huge increase in the surface area (or surface to volume ratio) of the material.
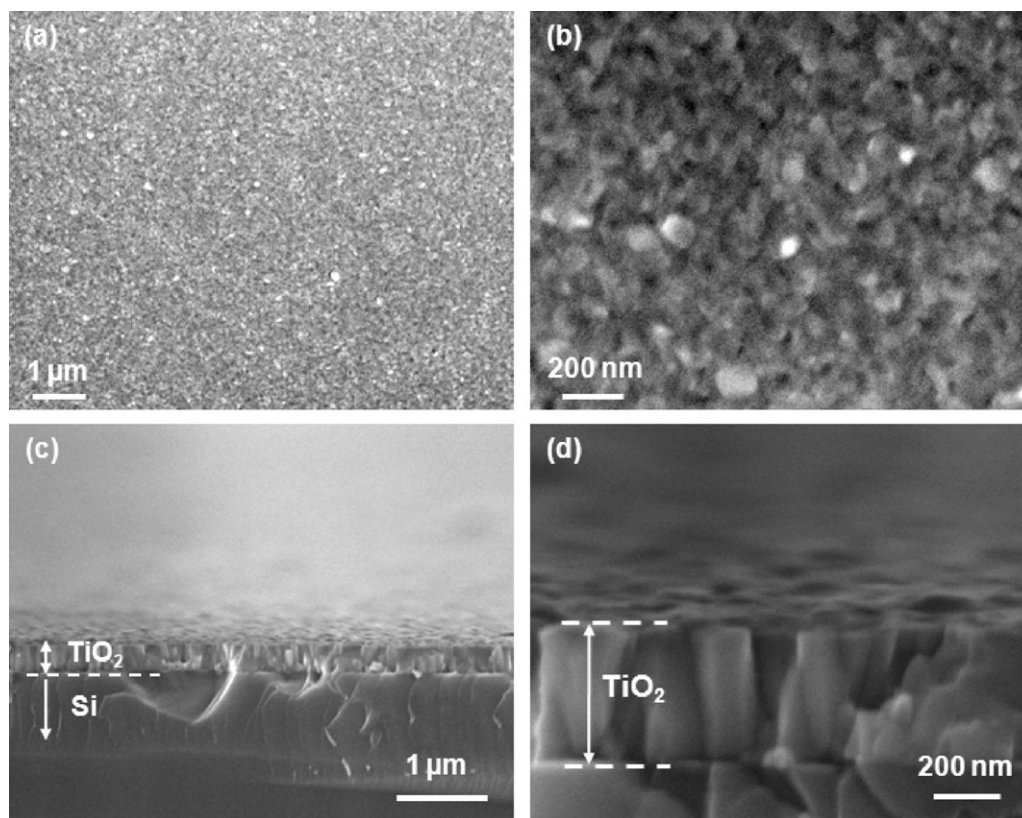
Fig. 2. SEM images of the surface morphology of the TiO$_2$ film deposited at 600 °C.

3.2. Preliminary investigation of CTC degradation

Experiments using direct photolysis (DP), photo-catalysis (PC), electro-oxidation (EO) and PECO processes were carried out in order to compare the CTC degradation efficiencies (Table 2). The

Fig. 3. X-ray diffraction patterns of TiO$_2$ film coated on Ti grids and on Si substrates at 600 °C.

DP process consisted in treating the effluent using only UV irradiation light at 254 nm, whereas in the PC process UV light was used in the presence of Ti/TiO$_2$ catalyst. The EO process was applied to treat the effluent using Ti/TiO$_2$ catalyst and Ti/Pt anode electrodes, while in the PECO process; the Ti/TiO$_2$ photoanode was used under UV irradiation and an external potential. The results of CTC degradation using different experimental conditions (tests T1–T8) are shown in Table 3. As it can be been seen from these data, the CTC degradation rate is higher using internal UV illumination (see the tests T2, T4, and T8). Only 16% of CTC was oxidized using DP process with external UV configuration. By comparison, 37% of CTC was removed by DP with internal UV illumination. In the case of direct photolysis, UV radiations absorbed by H$_2$O molecules allow the generation of powerful oxidizing species such as the hydroxyl radicals (OH$^\bullet$) and hydrogen peroxide (H$_2$O$_2$) [9,29]. The direct contact of UV light (internal UV illumination) with contaminated water induced high

Table 2
Different processes used for degradation of Chlortetracycline hydrochloride.

Parameters	Value	Process			
		PECO	PC	EO	DP
Intensity (A)	0.5	√		√	
Treatment time (min)	120	√	√	√	√
Light intensity (μW cm^{-2})	6900	√	√		√
UV lamp position	External	√	√		√
	Internal	√	√		√
Electrolyte (Na$_2$SO$_4$) (mol L^{-1})	0.05	√		√	
Type of Cathode	Inox	√		√	
Type of anode	Ti/Pt			√	
	Ti/TiO$_2$	√	√	√	
CTC (mol L^{-1})	0.05	√	√	√	√

DP, direct photolysis; PC, photocatalysis; EO, electro-oxidation; PECO, photoelectrocatalytic-oxidation.

Table 3
Chlortetracycline hydrochloride removal under various experimental conditions.

Processes	Tests	Intensity (A)	Times (min)	Anode	Cathode	Light intensity (mW cm^{-2})	UV lamp position	Electrolyte (Na$_2$SO$_4$ mol L^{-1})	CTC removal (%)
Parameters									
DP	T1	–	120	–	–	6.9	External	–	16
	T2	–	120	–	–	6.9	Internal	–	37
PC	T3	–	120	Ti/TiO$_2$	–	6.9	External	–	25
	T4	–	120	Ti/TiO$_2$	–	6.9	Internal	–	47
EO	T5	0.5	120	Ti/Pt	Inox	–	–	0.05	60.1
	T6	0.5	60	Ti/TiO$_2$	Inox	–	–	0.05	37.5
PECO	T7	0.5	120	Ti/TiO$_2$	Inox	6.9	External	0.05	80.9
	T8	0.5	120	Ti/TiO$_2$	Inox	6.9	Internal	0.05	81.2

DP, direct photolysis; PC, photocatalysis; EO, electro-oxidation; PECO, photoelectrocatalytic-oxidation.

oxidative degradation. The high CTC degradation using internal UV illumination can be due to the rapid increase of HO$^\bullet$ species concentration in the solution. The exposure of Ti/TiO$_2$ electrode under UV light (PC process) decreased the final CTC concentrations. The residual CTC concentrations recorded after 120 min of treatment were 25% and 47% under external and internal UV illumination, respectively. These results indicate that the system (UV and Ti/TiO$_2$ catalyst) is working in a photocatalytic regime. Furthermore, the degradation rate of CTC by EO process at a current intensity of 0.5 A was tested using Ti/Pt and Ti/TiO$_2$ as anodes. The final CTC concentration recorded using Ti/Pt anode was 60.1% (after 120 min) and 37.5% using Ti/TiO$_2$ anode (after 60 min) in the absence of UV light. The nature of the anode material used affected the ions conductivity in the solutions and influenced the performance of the system. In EO process, the conductivity of the solution affects the current efficiency, the cell voltage and the electrical energy consumed [30]. For the same current intensity imposed (0.5 A), Ti/Pt electrode used at the anode provided a relatively low electrical resistance of 14 Ω during 120 min of electrolysis, whereas a value of 60 Ω was recorded using Ti/TiO$_2$ anode electrodes during 60 min of electrolysis. The potential difference existing between the electrodes connected to the power supply increased from 9.4 V to 30 V using Ti/TiO$_2$ anode, whereas it varied from 5.8 V to 7 V using Ti/Pt anode. This situation may affect the treatment performance in a long-term experiment. It was the reason for which Ti/Pt was more effective than Ti/TiO$_2$ for CTC oxidation using EO process.

However, a higher degradation efficiency was recorded (above 80%) by PECO process using Ti/TiO$_2$ photoanode at 0.5 A. In PECO process, UV radiation activates Ti/TiO$_2$ photoanode by transferring electrons from the valance band (VB) to the conduction band (CB), while at the same time the applied external potential prevents the recombination of photo-generated electron–hole pairs. Thus, the efficiency of CTC degradation was enhanced. Finally, PECO process was selected for the next step of this study using the experimental factorial design methodology.

3.3. Effect of the experiment parameters on the CTC degradation using the experimental factorial design methodology

The results presented above allowed us to clearly define the experimental region for RSM to study CTC degradation using the PECO process. The influence of different variables: current intensity (U_1), treatment time (U_2) pollutant concentration (U_3), and UV lamp position (U_4) on the CTC removal was investigated using factorial matrix (2^k, k being the number of factors; k = 4). The experiment region investigated for CTC degradation and the code values are shown in Table 4. The experimental results are presented in Table 5. With this design it was possible to calculate the principle effect of each factor and the interaction between them. The experimental

response associated to a 2^4 factorial design (four variables) is represented by a linear polynomial model with interaction, as follows:

$$Y = b_0 + b_1X_1 + b_2X_2 + b_3X_3 + b_4X_4 + b_{12}X_1X_2 + b_{13}X_1X_3$$
$$+ b_{14}X_1X_4 + b_{23}X_2X_3 + b_{24}X_2X_4 + b_{34}X_3X_4 \qquad (1)$$

where Y represents the experimental response (CTC degradation); b_0 represents the average value of the responses of the 16 assays; X_i the coded variable (-1 or $+1$); b_i represents the principal effect of each factor i on the response and b_{ij} represents the interaction effect between factor i and factor j on the response. The coefficients of the model were calculated using the half-difference between the arithmetic average of the response values when the associated coded variable is at a level ($+1$) and the arithmetic average of the response values when the associated coded variable is at level (-1). Design-Expert® Program Software (Design Expert 7, Stat-Ease Inc., Minneapolis) was used to calculate the coefficient of the polynomial model.

$$Y = 50.85 + 12.06X_1 + 5.65X_2 - 2.73X_3 - 2.18X_4 - 0.36X_1X_2$$
$$+ 1.11X_1X_3 + 0.81X_1X_4 + 0.35X_2X_3 - 0.55X_2X_4 + 0.60X_3X_4$$
$$(2)$$

The value of the regression coefficient R^2 was 0.996. The coefficient b_0 = 50.85 represents the average value of the response of 16 assays. According to Eq. (2), it can also been seen that current intensity and treatment times have a positive effect on CTC degradation, whereas pollutant concentration and UV lamp position have a negative effect on CTC degradation. The interaction effects were globally weaker than the main effects.

The importance of the factors and interactions on CTC degradation has been put into evidence using Eq. (3). Indeed, it is possible to give more significant information by calculating the contribution of each factor on the response.

$$P_i = \left(\frac{b_i^2}{\sum b_i^2} \right) * 100 \quad (i \neq 0) \qquad (3)$$

where b_i represents the estimation of the principal effect of the factor i. Thus, it is found that the contribution of current intensity and treatment time on CTC removal is around 76.2% and 16.7%, respectively, whereas that of pollutant concentration and UV lamp position account only for 4.0% and 2.5%, respectively (Fig. 4).

With the exception of the interactions X_1X_3 (current intensity and pollutant concentration), the other interactions have a negligible effect. The interaction effect of X_1X_3 on CTC degradation is presented in Fig. 5. Each point represents the combination between two factors: current intensity and pollutant concentration. At current intensity of 0.5 A and 50 mg L^{-1} of CTC concentration, an average reduction of 61.3% was recorded (assays 7, 8, 15, and 16). When

Table 4
Data for optimization operation: experimental range and levels of independent process variables.

Coded variables (X_i)	Factor (U_i)	Experimental field		$U_{i,0}$	ΔU_i
		Min value (−1)	Max value (+1)		
X_1	U_1: Current intensity (A)	0.25	0.50	0.375	0.125
X_2	U_2: Electrolysis time (min)	60	120	90	30
X_3	U_3: CTC concentration (mg L^{-1})	25	50	37.5	12.5
X_4	U_4: UV lamp position	External	Internal	–	–

Table 5
Experimental factorial matrix in the 2^4 design.

Assays	Experiment design				Experiment plan				Result, Y degradation efficacy (%)
	X_1	X_2	X_3	X_4	U_1	U_2	U_3	U_4	
1	−1	−1	−1	−1	0.25 A	60 min	25	External	33.3
2	−1	+1	−1	−1	0.25 A	120 min	25	External	43.1
3	−1	−1	+1	−1	0.25 A	60 min	50	External	27.8
4	−1	+1	+1	−1	0.25 A	120 min	50	External	39
5	+1	−1	−1	−1	0.5 A	60 min	25	External	58.8
6	+1	+1	−1	−1	0.5 A	120 min	25	External	68
7	+1	−1	+1	−1	0.5 A	60 min	50	External	54.4
8	+1	+1	+1	−1	0.5 A	120 min	50	External	65
9	−1	−1	−1	+1	0.25 A	60 min	25	Internal	41.0
10	−1	+1	−1	+1	0.25 A	120 min	25	Internal	53.1
11	−1	−1	+1	+1	0.25 A	60 min	50	Internal	29.0
12	−1	+1	+1	+1	0.25 A	120 min	50	Internal	44
13	+1	−1	−1	+1	0.5 A	60 min	25	Internal	60
14	+1	+1	−1	+1	0.5 A	120 min	25	Internal	74.3
15	+1	−1	+1	+1	0.5 A	60 min	50	Internal	57.3
16	+1	+1	+1	+1	0.5 A	120 min	50	Internal	68.5

pollutant concentration (X_3) is fixed at the highest level (50 mg L^{-1}), current intensity has a significant influence on the removal of CTC. The degradation rate passed from 34.9% to 61.3% (a reduction gain of 27 units). When the pollutant concentration is fixed at the lowest level (25 mg L^{-1}), the degradation rate passed from 42.6% to 64.5% (a reduction gain of 22 units). Consequently, current intensity is a major factor that influences degradation rate of CTC, but it directly depends of pollutant concentration. In the PECO process, current intensity is a key factor that influences pollutant degradation efficiency. Current intensity supplied to the catalyzed Ti/TiO$_2$ electrode prevents the recombination of photo-generated electron–hole pairs (h$^+$/e$^-$) [31,32]. Therefore, the electrons and holes have more opportunities to participate in degradation of CTC pollutant directly on the surface of nanostructured Ti/TiO$_2$ photo-anode (adsorption) or indirectly by reacting with active species (such as hydroxyl radicals) [16]. Furthermore, the PECO process was more effective at low CTC concentrations (25 mg L^{-1}). This result indicates that CTC degradation reaction is limited by the amount of reactive species (OH$^\bullet$ radicals) produced by UV illumination. At higher pollutant concentration, the reactive species are insufficient for enhance degradation efficiency [33]. According to

Wang et al. [33], the decrease in pollutant degradation efficiency can be attributed to the competition reaction between intermediate products for reacting with hydroxyl radicals. The influence of initial concentration of pollutant was also put into evidence by Ding et al. [34] while studying photoelectrocalytic degradation of benzotriazole. The degradation experiments were carried out at different initial concentrations (from 0.05 mM to 0.5 mM) in 0.5 M of Na$_2$SO$_4$ using a voltage of 0.8 V. The degradation efficiency was around 40% at initial concentration of 0.5 mM, whereas more than 99% of benzotriazole was removed at initial concentration of 0.05 mM. The decrease in degradation rate of pollutant while increasing the initial concentration increase can be explained in two ways. Firstly, the reaction between photogenerated holes (or hydroxyl radicals) and pollutant can be inhibited owing to adsorbed pollutant on the surface of the catalyst. Secondly, the UV radiations may be more adsorbed by pollutants rather than photocatalysts Ti/TiO$_2$ and consequently limits the catalytic reaction efficiency [34].
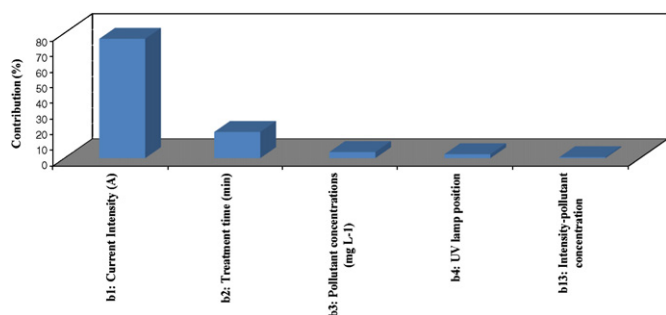
Fig. 4. Graphical Pareto analysis of the effect of current intensity, treatment time, pollutant concentration, and UV lamp position on CTC degradation.
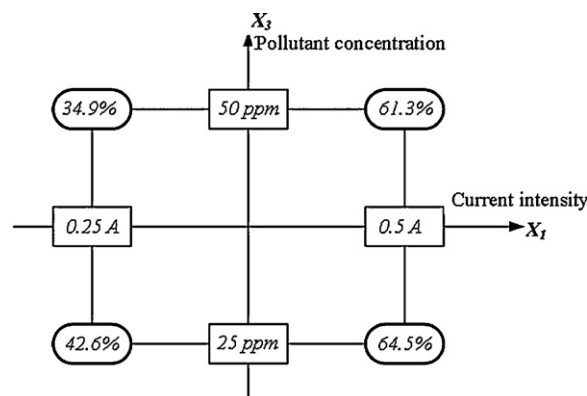
Fig. 5. Interaction $X13$ between current intensity and pollutant concentration.

Table 6
Central composite matrix and experimental results.

Experiment number	Experimental design			Experimental plan			Result, Y degradation efficacy (%)
	X_1	X_2	X_3	U_1	U_2	U_3	
For external UV lamp (U_4)							
17	−1.68	0	0	0.16	90	37.50	31.4
18	1.68	0	0	0.59	90	37.50	62.5
19	0	−1.68	0	0.38	39.55	37.50	33.3
20	0	1.68	0	0.38	140.45	37.50	59.7
21	0	0	−1.68	0.38	90	16.48	57.8
22	0	0	1.68	0.38	90	58.52	52.2
23	0	0	0	0.38	90	37.50	55
24	0	0	0	0.38	90	37.50	55.0
25	0	0	0	0.38	90	37.50	55.8
26	0	0	0	0.38	90	37.50	55.8
27	0	0	0	0.38	90	37.50	55.2
28	0	0	0	0.38	90	37.50	55.5
For internal UV lamp (U_4)							
29	−1.68	0	0	0.16	90	37.50	39.6
30	1.68	0	0	0.59	90	37.50	67.3
31	0	−1.68	0	0.38	39.55	37.50	45.5
32	0	1.68	0	0.38	140.45	37.50	61.7
33	0	0	−1.68	0.38	90	16.48	60.7
34	0	0	1.68	0.38	90	58.52	57.2
35	0	0	0	0.38	90	37.50	59.6
36	0	0	0	0.38	90	37.50	58.8
37	0	0	0	0.38	90	37.50	58.4
38	0	0	0	0.38	90	37.50	58.7
39	0	0	0	0.38	90	37.50	58.9
40	0	0	0	0.38	90	37.50	59.4

Finally, the factorial plan design was used to determine the interactions affecting the response and indicates that if the lowest or the highest levels of the factors are favourable or not. The results show that the response is greatly influenced by the factors having a significant effect. However, the factorial plan design cannot be used to determine the optimal conditions of CTC degradation. For this reason, a RSM should be used in a second step to determine the optimal conditions for CTC degradation.

3.4. Optimization conditions for CTC degradation using central composite design (CCD) methodology

A two-level central composite experimental design, with six replicates at the center point leading to a total number of forty experiments was used for response surface modeling (Table 6). For the evaluation of experimental data, the response was described by a second-order model in the form of quadratic polynomial equation given below:

$$Y = b_0 + \sum_{i=1}^{k} b_i.X_i + \sum_{i=1}^{k} b_{ii}.X^2 + \sum_{j}\sum_{i=2}^{k} b_{ij}.X_iX_j + e_i \quad (4)$$

where Y is the experimental response; X_i and X_j are the independent variables; b_0 is the average of the experimental response; b_i is the estimation of the principal effect of the factor j on the response Y; b_{ii} is the estimation of the second effect of the factor i on the response Y; b_{ij} is the estimation of the interaction effect between i and j on the response Y and e_i represents the error on the response Y. All coefficients are calculated using the least square method [19]:

$$B = (X^TX)^{-1}X^TY \quad (5)$$

where B represents the vector of estimates of the coefficients; X is the model matrix, and Y is the vector of the experiment results. The variables (X_i) are coded according to the following equation [35]:

$$X_i = \frac{U_i - U_{i0}}{\Delta U_i} \quad (6)$$

where $U_{i,0} = (U_{i,\max} + U_{i,\min})/2$ represents the value of U_i at the center; $\Delta U_i = (U_{i,\max} - U_{i,\min})/2$ is the value of variable change step and $U_{i\max}$ and $U_{i\min}$ are the maximum and the minimum values of the effective variable U_i, respectively. The coefficients of the polynomial model (quadratic model) were calculated using the Design-Expert® Program Software:

For Internal UV lamp:

$$Y_1 = -23.0807 + 193.235X_1 + 0,7462X_2 - 0.3788X_3$$
$$- 0.0966X_1X_2 0.712X_1X_3 + 0.000933X_2X_3 - 174.967X_1^2$$
$$- 0.003095X_2^2 - 0.00216X_3^2 \quad (7)$$

For external UV lamp:

$$Y_1 = -34.93077 + 204.20030X_1 + 0.76658X_2 - 0.34325X_3$$
$$- 0.0966X_1X_2 0.712X_1X_3 + 0.000933X_2X_3 - 174.967X_1^2$$
$$- 0.003095X_2^2 - 0.00216X_3^2 \quad (8)$$

From these Eqs. ((7) and (8)), it can be seen that current intensity is very meaningful for CTC degradation using both internal and external UV position. Current intensity and treatment time are positive effect on the response compared to pollutant concentration, which has a negative effect on the removal of CTC. The predicted contour plots (curves of constant response) and the three-dimensional representation of the same plots are given in Fig. 6. This figure clearly shows that CTC removal efficiency increased with increasing current intensity at all pollutant concentrations studied varying from 25 to 50 mg L^{-1} (for internal UV position). 63% CTC removal efficiency could be achieved at constant treatment time of 90 min (treatment time at the center of the experimental region investigated) while the current intensity was above 0.40 A for all concentrations of pollutant investigated varying from 25 to 50 mg L^{-1}. From the correlation between the current intensity
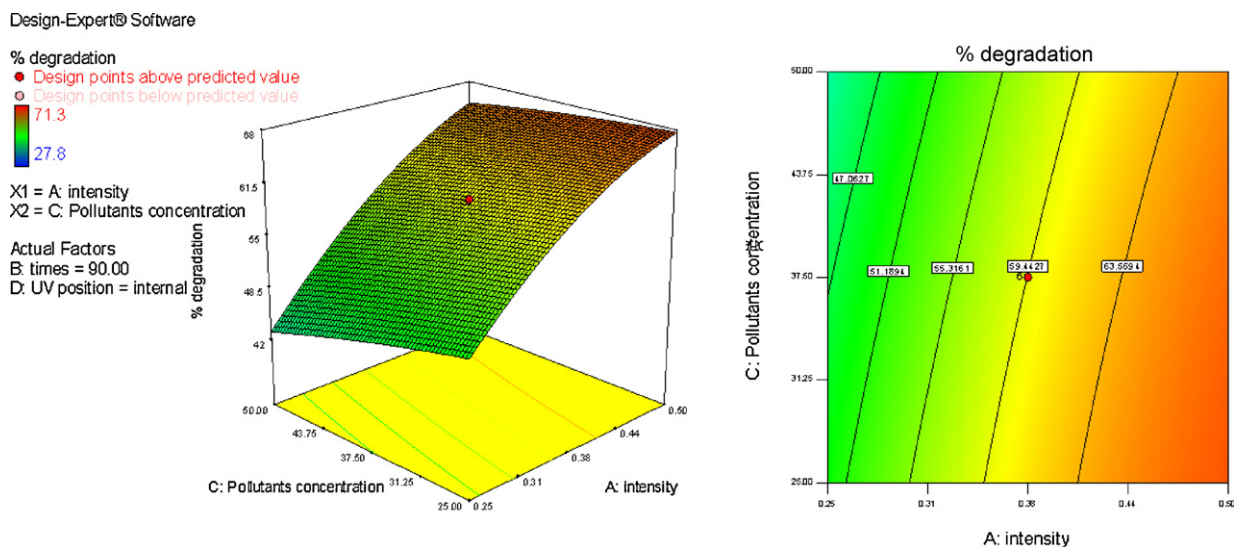
Fig. 6. The effect of current intensity (A) and pollutant concentration (mg L^{-1}) on CTC removal (application time: 90 min) three-dimensional plot; results obtained from central composite matrix.
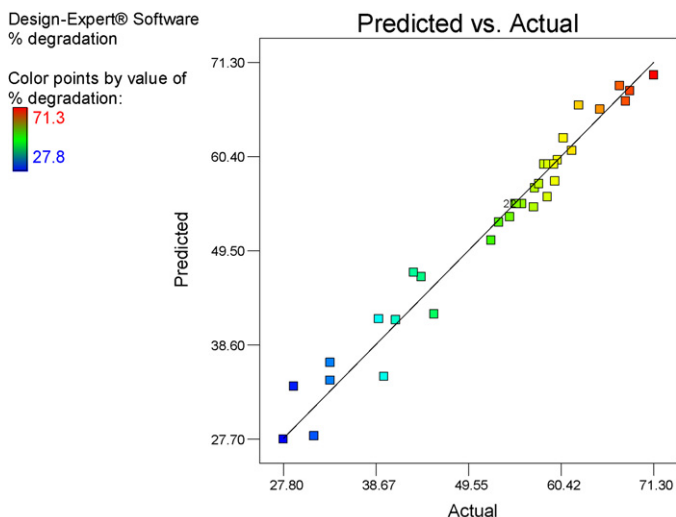
Table 7
ANOVA results for the response surface quadratic for CTC degradation.

Source	Analysis of variance				
	d.f.[a]	Sum of square	Mean of square	F-value	Pr > F
Model	13	4857.49	373.65	60.04	<0.0001
Residual	26	161.82	6.22	–	–
Lack of fit	16	160.12	10.01	58.81	<0.0001
Pure error	10	1.70	0.17	–	–

[a] Degree of freedom; F: Fisher coefficient; $R^2 = 0.9678$.

and pollutant concentration, it can be concluded that the current intensity has more significant impact on CTC removal efficiency.

The comparison between actual (experimental) and predicted values of CTC degradation are presented in Fig. 7. An agreement between actual and predicted values of CTC degradation is satisfactory and in accordance with the statistical significance of the quadratic model. Table 7 shows the analysis of variance (ANOVA) of regression parameters of the predicted response surface quadratic model for CTC removal using PECO process. As it can be seen from this table, the model F-value of 60.04 and a low probability

value (Pr > F = 0.0001) indicate that the model is significant for CTC removal. The value of the correlation coefficient ($R^2 = 0.9678$) indicates that only 3.22% of the total variation could not be explained by the empirical model. According to [36], R^2 should be at least 0.80 for a good fit of a model. The R^2 value (0.9678) recorded in the present study for CTC removal was higher than 0.80, indicating that the regression model explained the reaction well.

The main objective of the optimization is to determine the optimum values for CTC removal using the PECO process. The criteria selected for the optimization condition for CTC degradation are the following: (i) current intensity and pollutant concentration have to be minimized; (ii) treatment time has to be maximized, and (iii) UV lamp position was investigated in the experimental range. The optimization results of the process variables for CTC removal are shown in Table 8. The desirability function value was found as 0.905 for these optimum conditions. The theoretical response proposed by Design-Expert® Program Software for CTC degradation was 72.7%. To confirm the model adequacy and the validity of the optimization procedure, additional experiments were performed under optimal operating conditions. The average value of the experimental response measured using UV–vis absorption spectrophotometer is

Fig. 7. Comparison between actual and predicted values for CTC degradation.

Table 8
Determination of optimum operating conditions proposed by Design-Expert® Program Software.

Parameter	Optimum value
Applied electric current (A)	0.39
Treatment time (min)	120
Pollutant concentration (mg L^{-1})	25
UV lamp position	Internal
Experimental response (%)	74.2 ± 0.57
Theoretical response (%)	72.73

74.2% ± 0.57%. This CTC degradation rate of ∼74% was recorded at the end of this experiment, and is found to be very close to the value proposed by the model (72% of CTC degradation).

However, experimental results determined using liquid chromatography mass spectrometer (LC/MS/MS) shows that the removal of CTC is around 97% ± 1.12%. UV–vis absorption spectrophotometer is an indirect analytical method. According to Beer–Lambert law, the measure of the concentration of species can be determined from the measured absorbance. The presence of interfering substance can influence the absorption spectrum and consequently can modify the results. By comparison, LC/MS/MS technique, which combines simultaneously a powerful physical separation technique and a powerful technique of analysis and mass detection has a very high sensitivity and selectivity towards several antibiotics [37]. It is worth noting that during the treatment, the pH varied from 4.82 ± 0.14 (initial value) to 7.67 ± 0.42. This variation could be probably attributed to by-products formation during the application of the PECO process. It is worth noting that hydroxyl radical produced at the surface of photo-anode could react with the CTC and lead to the formation of by-products. Subsequently, by-products can be oxidized by hydroxyl radical into further intermediates including ring-opened structures. The above mentioned hypothesis of intermediates and CO_2 formation was based on the results described elsewhere using hydroxyl radical as oxidant agent [38]. According to Halling-Sørensen et al. [8], the possible formation of by-products derived from CTC oxidation are: 5a,6-anhydrochlorotetracycline hydrochloride (ACTC); 4-epi-chlorotetracycline hydrochloride (ECTC); 4-epi-anhydro-chlorotetracycline hydrochloride (EACTC); iso-chlorotetracycline (iso-CTC); keto-chlorotetracycline (keto-CTC). At pH value between 3 and 6.5, ECTC, EACTC, ACTC, and keto-CTC are the predominant forms, while at pH value between 6.5 and 9, iso-CTC, keto-CTC (more predominate at this pH interval), demethylation of the isochlorotetracycline (DM-iso CTC) are the predominant ones. The pH, ions, and solvents clearly influence the predominant forms of CTC by-products present in the solution [8]. In our study, the initial pH value of the CTC solution was 4.82 ± 0.14. This result demonstrates clearly that the by-products were formed after photoelectrocatalytic treatment of CTC solution. The by-products of CTC can interfere on the absorption spectrum of CTC and modify the removal rate of CTC during electrolysis. Photoelectrocatalytic treatment costs of CTC (including only chemical consumption and energy consumption) recorded in the best experimental condition was estimated to $4.55 ± 0.01 m^{-3}$.

It is to be underlined that, sometimes by-products can be as toxic as the initial pollutant or more toxic than that the initial pollutant. To circumvent these drawbacks, by-products have to be further oxidized into water and carbon dioxide. In view of enhancing CTC removal and to avoid possible toxicity of treated-effluent, an additional parameter (X_5) such as the type of supporting electrolyte (NaCl and Na_2SO_4) should be tested. Indeed, on Ti/TiO_2 photo-anode, chloride ions can be oxidized and form hypochlorous acid (HClO) in solution. HClO is powerful oxidant capable of oxidizing and modifying the structure of organic molecules [39,40] and leading to more oxidized and less toxic compounds. However, this alternative has to be carefully studied because of the possible formation of organochlorinated compounds, which can be more toxic than the initial pollutant.

Another interesting alternative could be the use of another type of cathode material, such as vitreous carbon (VC) versus stainless steel (SS). It has been demonstrated that, on vitreous carbon electrode, hydrogen peroxide (H_2O_2) can be electrochemically generated by cathodic reduction of dissolved oxygen [41]. This peroxide induces non offensive by-products contrarily to chlorine. Under UV irradiation, hydrogen peroxide can be decomposed into hydroxyl radical (in addition to hydroxyl radical produced on

the surface of photocatalyst). This should contribute to enhance CTC degradation. Likewise, the addition of an electron acceptor (e.g. H_2O_2) should prevent the electron-hole recombination and increase the photocatalyst efficiency [42]. According to previous studies [41,43,34], such an oxidant agent (H_2O_2) is beneficial for photocatalytic reaction by trapping the conduction band electron in order to generate more hydroxyl radical.

4. Conclusion

In this study, the Ti/TiO_2 rectangular electrode was prepared by a PLD method. It showed that the TiO_2 coating at 600 °C is very uniform in thickness and was found to be of rutile structure. By investigating the photoelectrocatalytic degradation process of CTC in aqueous medium using this electrode, current intensity and treatment time were found to be the most influent parameters. The contribution of current intensity and treatment time were 76.2% and 16.7%, respectively, while the contribution of pollutant concentration and UV lamp position represented only 4% and 2.5%, respectively. A central composite design was employed to define the optimal operating condition for CTC removal. Current intensity is very meaningful for CTC degradation using both internal and external UV lamp configuration. Current intensity and treatment time have positive effects on the response compared to the pollutant concentration which has a rather negative one on the removal of CTC. The PECO process applied under optimal conditions (at current intensity of 0.39 A during 120 min with internal position of the UV lamp) is able to oxidize around 74.2 ± 0.57%, of CTC.

However, in view of enhancing CTC removal and to avoid possible toxicity of treated-effluent, another type of cathode material such as vitreous carbon (VC) should be tested. On such a cathode electrode, hydrogen peroxide (H_2O_2) can be electrochemically generated and decomposed into hydroxyl radical under UV irradiation. Likewise, the identification of by-products needs to be rigorously verified and a mechanism of CTC degradation should be proposed. The total organic carbon (TOC) should be measured to evaluate the level of the degradation and see if CTC is completely or partially transformed into water and carbon dioxide.

References

[1] J.J. Lòpez-Penalver, M. Sànchez-Polo, C.V. Gòmez-Pacheco, J. Rivera-Utrilla, Photodegradation of tetracyclines in aqueous solution by using UV and UV/H_2O_2 oxidation processes, J. Chem. Technol. Biotechnol. 85 (10) (2010) 1325–1333.
[2] J. Tolls, Sorption of veterinary pharmaceuticals in soils: a review, Environ. Sci. Technol. 35 (2001) 3397–3406.
[3] D.W. Kolpin, E.T. Furlong, M.T. Meyer, E.M. Thurman, S.D. Zaugg, L.B. Barber, H.T. Buxton, Pharmaceuticals, hormones, and other organic wastewater contaminants in U.S. streams, 1999–2000: a national reconnaissance, Environ. Sci. Technol. 36 (2002) 1202–1211.
[4] X. Miao, F. Bishay, M. Chen, C.D. Metcalfe, Occurrence of antimicrobials in the final effluents of wastewater treatment plants in Canada, Environ. Sci. Technol. 38 (2004) 3533–3541.
[5] K. Kuemmerer, Significance of antibiotics in the environment, J. Antimicrob. Chemother. 52 (1) (2003) 5–7.
[6] T. Heberer, Occurrence, fate, and removal of pharmaceutrical residues in the aquatic environment: a review of recent research data, Toxicol. Lett. 131 (1–2) (2002) 5–17.
[7] J. Jeong, W. Song, W.J. Cooper, J. Jung, J. Greaves, Degradation of tetracycline antibiotics: mechanisms and kinetic studies for advanced oxidation/reduction processes, Chemosphere 78 (2010) 533–540.
[8] B. Halling-Sørensen, G. Sengeløv, J. Tjørnelund, Toxicity of tetracyclines and tetracycline degradation products to environmentally relevant bacteria including selected tetracycline-resistant bacteria, Arch. Environ. Contam. Toxicol. 42 (3) (2002) 263–271.

[9] I. Kim, H. Tanaka, Photodegradation characteristics of PPCPs in water with UV treatment, Environ. Int. 35 (2009) 793–802.

[10] I.R. Bautitz, R.F.P. Nogueira, Degradation of tetracycline by photo-Fenton process-Solar irradiation and matrix effects, J. Photochem. Photobiol. A 184 (2007) 141–146.

[11] T. Zhang, M. Zhang, X. Zhang, H.H. Fang, Tetracycline resistance genes and tetracycline resistant lactose-fermenting enterobacteriaceae in activated sludge of sewage treatment plants, Environ. Sci. Technol. 438 (2009) 3455–3460.

[12] C. Reyes, J. Fernandez, J. Freer, M.A. Mondaca, C. Zaror, S. Malato, H. Mansilla, Degradation and inactivation of tetracycline by TiO_2 photocatalysis, J. Photochem. Photobiol. A 184 (2006) 141–146.

[13] F. Ingerslev, B. Halling-Sorensen, Importance of the test volume on the lag phase in biodegradation studies, Environ. Toxicol. Chem. 19 (10) (2000) 2443–2447.

[14] K. Kummerer, T.S. Hartmann, M. Meyer, Biodegradability of the anti-tumor agent ifosfamide and its occurrence in hospital effluents and communal sewage, Water Res. 31 (11) (1997) 2705–2710.

[15] R.P. Rey, A.S. Padron, P.L. Leon, M.M. Pozo, C. Baluja, Ozonation of cytostatics in water medium. Nitrogen bases, Ozone Sci. Eng. 21 (1999) 69–77.

[16] C. Adams, M.Y. Wang, K. Loftin, M. Meyer, Removal of antibiotics from surface and distilled water in conventional water treatment processes, J. Environ. Eng. Div. ASCE 128 (2002) 253–260.

[17] L. Ji, W. Chen, L. Duan, D. Zhu, Mechanisms for strong adsorption of tetracycline to carbon nanotubes: a comparative study using activated carbon and graphite as adsorbents, Environ. Sci. Technol. 43 (2009) 2322–2327.

[18] C.A. Martinez-Huitle, S. Ferro, Electrochemical oxidation of organic pollutants for the wastewater treatment: direct and indirect processes, Chem. Soc. Rev. 35 (2006) 1324–1340.

[19] R.H. Myers, D.C. Montgomery, Response Surface Methodology: Process and Product Optimization using Designed Experiments, 2nd ed., John Wiley and Sons, New York, NY, 2002.

[20] E. Desbiens, M.A. El Khakani, Growth of high-K silicon oxynitride thin films by means of a pulsed laser deposition-atomic nitrogen plasma source hybrid system for gate dielectric applications, J. Appl. Phys. 94 (9) (2003) 5969–5975.

[21] Z. Qiang, C. Adams, Potentiometric determination of acid dissociation constants (pK_a) for human and veterinary antibiotics, Water Res. 38 (2004) 2874–2890.

[22] Z. Zaroual, H. Chaair, A.H. Essadki, K. El Ass, M. Azzi, Optimizing the removal of trivalent chromium by electrocogulation using experimental design, Chem. Eng. J. 148 (2009) 488–495.

[23] R.S. Khandpur, Handbook of Analytical Instruments, 2nd ed., Tata Mc Graw-Hill, 2006.

[24] S.i. Kitazawa, Y. Choi, Sh. Yamamoto, T. Yamaki, Rutile and anatase mixed crystal TiO_2 thin film prepared by pulsed laser deposition, Thin Solid Films 515 (4) (2006) 1901–1904.

[25] A. Jaroenworaluck, D. Regonini, C.R. Bowen, R. Stevens, A microscopy study of the effect of heat treatment on the structure and properties of anodized TiO_2 nanotubes, Appl. Surf. Sci. 256 (2010) 2672–2679.

[26] D. Regonini, A. Jaroenworaluck, R. Stevens, C.R. Bowen, Effect of heat treatment on the properties and structure of TiO_2 nanotubes: phase composition and chemical composition, Surf. Interface Anal. 42 (2010) 139–144.

[27] A. Guinier, Théorie et Technique de la radiocristallographie, 3rd ed., Dunod, Paris, 1962.

[28] C.-S. Kim, I.-M. Kwon, B.K. Moon, J.H. Jeong, B.-C. Choi, J.H. Kim, H. Choi, S.S. Yi, D.-H. Yoo, K.-S. Hong, J.-H. Park, H.S. Lee, Synthesis and particle size effect on the phase transformation of nanocrystalline TiO_2, Mater. Sci. Eng. C 27 (2007) 1343–1346.

[29] G. Heit, A. Neuner, P.Y. Saugy, A.M. Braun, Vacuum-UV (172 nm) actinometry – the quantum yield of the photolysis of water, J. Phys. Chem. A 102 (1998) 5551–5561.

[30] N. Daneshvar, A. Oladegaragoze, N. Djafarzadeh, Decolorization of basic dye solutions by electrocoagulation: an investigation of the effect of operational parameters, J. Hazard. Mater. B129 (2006) 116–122.

[31] G. Waldner, M. Pourmodjib, R. Bauer, M. Neumann-Spallart, Photoelectrocatalytic degradation of 4-chlorophenol and oxalic acid on titanium dioxide electrodes, Chemosphere 50 (2003) 989–998.

[32] X.Z. Li, F.B. Li, C.M. Fan, Y.P. Sun, Photoelectrocatalytic degradation of humic acid in aqueous solution using a Ti/TiO_2 mesh photoelectrode, Water Res. 36 (2002) 2215–2224.

[33] N. Wang, X. Li, Y. Wang, X. Quan, G. Chen, Evaluation of bias potential enhanced photocatalytic degradation of 4-chlorophenol with TiO_2 nanotube fabricated by anodic oxidation method, Chem. Eng. J. 146 (2009) 30–35.

[34] Y. Ding, C. Yang, L. Zhu, J. Zhang, Photoelectrochemical activity of liquid phase deposited TiO_2 film for degradation of benzotriazole, J. Hazard. Mater. 175 (2010) 96–103.

[35] M. Tir, N. Moulai-Mostefa, Optimization of oil removal from oily wastewater by electrocoagulation using response surface method, J. Hazard. Mater. 158 (2008) 107–115.

[36] A.M. Joglekar, A.T. May, Product excellence through design of experiments, Cereal Foods World 32 (1987) 857–868.

[37] F. Hernàndez, V.J. Sancho, M. Ibànez, C. Guerrero, Antibiotic residue determination in environmental waters by LC–MS, TrAC, Trends Anal. Chem. 26 (6) (2007) 466–485.

[38] L. Tran, P. Drogui, G. Mercier, J.F. Blais, Comparison between Fenton oxidation process and electrochemical oxidation for PAH removal from an amophoteric surfactant solution, J. Hazard. Mater. 40 (2010) 1493–1510.

[39] P. Drogui, J.F. Blais, G. Mercier, Review of electrochemical technologies for environmental applications, Recent Patent Eng. 1 (2007) 257–272.

[40] P. Canizares, J. Lobato, R. Paz, C.J. Saez et, M.A. Rodrigo, Electrochemical oxidation of phenolic wastes with boron-doped diamond anodes, Water Res. 39 (2005) 2687–2703.

[41] Y.B. Xie, X.Z. Li, Degradation of bisphenol A in aqueous solution by H_2O_2-assisted photoelectrocatalytic oxidation, J. Hazard. Mater. B138 (2006) 526–533.

[42] R.R. Ozer, J.L. Ferry, Investigation of the photocatalytic activity of TiO_2–polyoxometalate systems, Environ. Sci. Technol. 35 (2001) 3242–3246.

[43] M.R. Sohrabi, M. Ghavami, Comparison of direct yellow 12 dye degradation efficiency using UV/semiconductor and UV/H_2O_2/semiconductor systems, Desalination 252 (2010) 157–162.